Controlling chaos with localized heterogeneous forces in oscillator chains

Ricardo Chacón
Departamento de Física Aplicada, Escuela de Ingenierías Industriales, Universidad de Extremadura, Apartado Postal 382, E-06071 Badajoz, Spain
(Received 20 April 2006; published 2 October 2006)

The effects of decreasing the impulse transmitted by localized periodic pulses on the chaotic behavior of homogeneous chains of coupled nonlinear oscillators are studied. It is assumed that when the oscillators are driven synchronously, i.e., all driving pulses transmit the same impulse, the chains display chaotic dynamics. It is shown that decreasing the impulse transmitted by the pulses of the two free end oscillators results in regularization with the whole array exhibiting frequency synchronization, irrespective of the chain size. A maximum level of amplitude desynchrony as the pulses of the two end oscillators narrow is typically found, which is explained as the result of two competing universal mechanisms: desynchronization induced by localized heterogeneous pulses and oscillation death of the complete chain induced by drastic decreasing of the impulse transmitted by such localized pulses. These findings demonstrate that decreasing the impulse transmitted by localized external forces can suppress chaos and lead to frequency-locked states in networks of dissipative systems.

DOI: 10.1103/PhysRevE.74.046202 PACS number(s): 05.45.Xt, 05.45.Pq, 87.18.Bb, 74.81.Fa

Understanding synchronization and desynchronization phenomena in networks of coupled oscillators [1] is currently a focus of research in physics [2], biology [3], and technology [4]. A fundamental problem closely related to the synchronization–desynchronization transition in the context of chaotic arrays is the control of chaos [5]. In this regard, previous studies have shown that chaos in coupled arrays of damped, periodically forced, nonlinear oscillators can be tamed by parametric disorder [6], impurities [7], localized controlling resonant forces [8,9], random shortcuts [10], and global disordered driving forces [11]. Usually, the arrays studied have been assumed to have homogeneous forces. In real-world systems, however, the periodic forces acting on the oscillators often exhibit heterogeneous distributions having different amplitudes and periods as well as different wave forms. In this work, I discuss the heterogeneity-induced regularization of homogeneous chains of coupled chaotic oscillators by decreasing the impulse transmitted by the driving forces acting on a *minimal* number of oscillators. As the transmitted impulse is decreased, the emergence of regular, frequency-locked dynamics typically occurs, while desynchronization is due to the dispersion in the oscillator's amplitude. For sufficiently small transmitted impulse, the phenomenon of oscillation death (quenching) typically occurs, irrespective of the chain size. For the sake of clarity, the findings are discussed through the analysis of one-dimensional chains of damped kicked rotators. The chain is described by the equations of motion

$$\ddot{\theta}_n + F\mathrm{cn}^2(\Omega t;m)\sin\theta_n = -\delta\dot{\theta}_n + k(\theta_{n+1} + \theta_{n-1} - 2\theta_n),$$

$$\ddot{\theta}_i + F\mathrm{cn}^2(\Omega t;m)\sin\theta_i = -\delta\dot{\theta}_i, \qquad (1)$$

where $n=2,\ldots,N-1$, $i=1,\ N$, $\Omega=\Omega(T,m)\equiv 2K(m)/T$, T and F are the forcing period and amplitude, respectively, δ is the damping coefficient, k is the coupling constant, $\mathrm{cn}(\cdot;m)$ is the Jacobian elliptic function of parameter m, $K(m)$ is the complete elliptic integral of the first kind, and where the *shape* parameter is taken as $m=0$ except for the two end rotators that are subjected to pulses of variable width ($m \in [0,1]$). The wave form of the pulse is varied by solely changing m between 0 and 1, such that by increasing m the pulse becomes narrower, and for $m \simeq 1$ one recovers a periodic sharply kicking excitation very close to the periodic δ function, but with finite amplitude and width as in real-world impacts (see Fig. 1). Observe that $\mathrm{cn}^2\ (\Omega t;m=0) = \cos^2(\pi t/T)$, while in the other limit, $m=1$, the pulse area vanishes. The Hamiltonian version of an isolated kicked rotator subjected to trigonometric pulses [$\delta=k=m=0$, cf. Eq. (1)] has been previously used to describe the center-of-mass motion of cold cesium atoms in an amplitude-modulated standing wave of light [12]. Equation (1) can be written in terms of the scaled dimensionless time $\tau \equiv t\sqrt{F}$. This scaling serves to stress that there are only four independent parameters in this model: the number of rotators N, the scaled period $T_F \equiv T\sqrt{F}$, the scaled damping coefficient $\delta_F \equiv \delta/\sqrt{F}$, and the scaled coupling constant $k_F \equiv k/F$. For the parameter values used in the present numerical simulations ($T_F=5.52$, $\delta_F=0.2$), each isolated rotator driven by trigonometric pulses ($m=0$) displays chaotic behavior characterized by a positive Lyapunov exponent [13]. Equation (1) was numerically integrated using a fourth-order Runge-Kutta algorithm with a

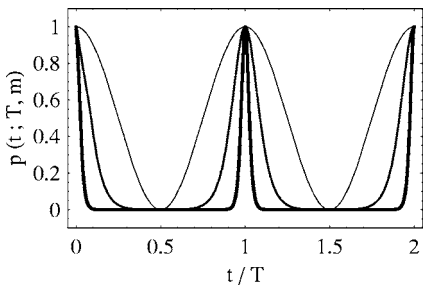

FIG. 1. Pulse function $p(t;T,m) \equiv \mathrm{cn}^2(2K(m)t/T;m)$ [cf. Eq. (1)] vs t/T for $m=0$ (thin line), $m=0.9993$ (medium line), and $m=1-10^{-14}$ (thick line). The quantities plotted are dimensionless.

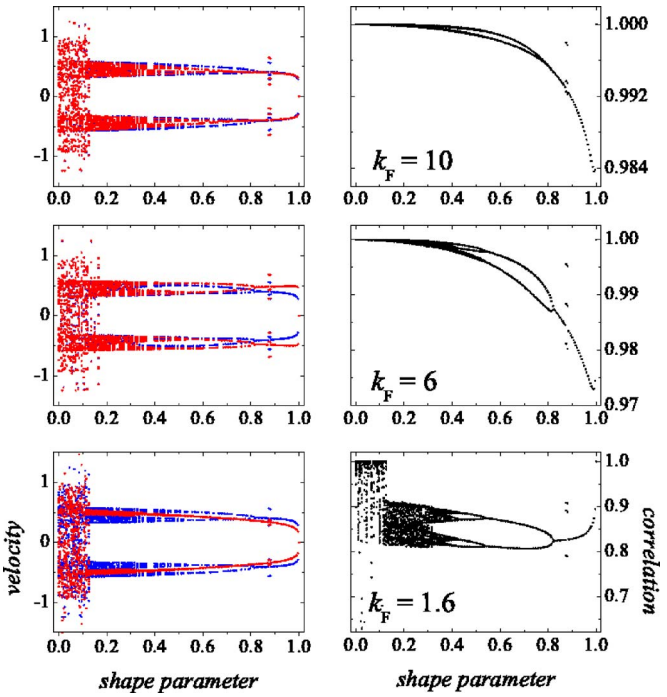

FIG. 2. (Color online) Bifurcation diagrams of angular velocities of the end [blue (black)] and central [red (gray)] rotators and correlation function as functions of the shape parameter for a chain of $N=9$ rotators and three values of the coupling. The quantities plotted are dimensionless.

time step $d\tau=0.001$. To visualize the global spatiotemporal dynamics of chains, one calculates the average velocity

$$\sigma(jT_F) \equiv \frac{1}{N}\sum_{n=1}^{N} \frac{d\theta_n}{d\tau}(jT_F), \tag{2}$$

where j is an integer multiple of the pulse period T_F, while the degree of synchronization is characterized by the correlation function

$$C(jT_F) \equiv \frac{2}{N(N-1)}\sum_{(il)} \cos\langle \theta_i(jT_F) - \theta_l(jT_F)\rangle, \tag{3}$$

where the summation is over all pairs of rotators. Note that $C(\tau)$ is 1(0) for the perfectly synchronized (desynchronized) state.

Figure 2 shows the angular velocities of the first [blue (black)] and central [red (gray)] rotators as well as the correlation function at $\tau=970T_F,\ldots,1000T_F$ vs the shape parameter for a chain of nine rotators. Typically, the individual rotators go from chaos to stable equilibrium (oscillator death) as the shape parameter increases from 0 to 1 while the whole chain goes from perfect synchrony (at $m=0$) to perfect trivial synchrony (at $m=1$) passing through desynchronized states for $m \in]0,1[$. The evolution of the desynchronized states is characterized by the correlation function undergoing an inverse period-doubling route as the shape parameter is increased, which is preceded by an inverse interior crisis when the coupling is sufficiently small (as for $k_F=1.6$, cf. Fig. 2). While the strength of desynchronization generally

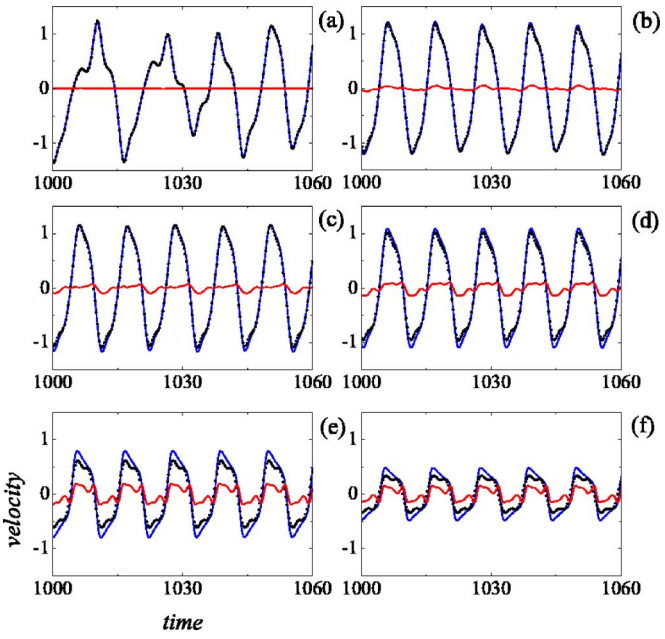

FIG. 3. (Color online) Angular velocities (arbitrary units) of the end [blue (black) line] and central (dots) rotators and their respective differences [red (gray) line] as a function of time (arbitrary units) for a chain of $N=3$ rotators, coupling $k_F=0.5$, and shape parameters: (a) $m=0$; (b) $m=0.3$; (c) $m=0.5$; (d) $m=0.8$; (e) $m=0.9892 \simeq m_{\min}$; (f) $m=0.999$.

diminishes as coupling is increased, as expected, one typically finds that the correlation function exhibits a minimum as a function of the shape parameter (at $m_{\min}$) for sufficiently large coupling values (as for $k_F=6$, 10, cf. Fig. 2). At this minimum, all rotators present a $2T_F$ periodic solution while their amplitude distribution reaches a maximum range, as in the example shown in Fig. 3. Thus the increase in the shape parameter has a double effect on the chaotic chains, which permits one to understand the appearance of a maximum

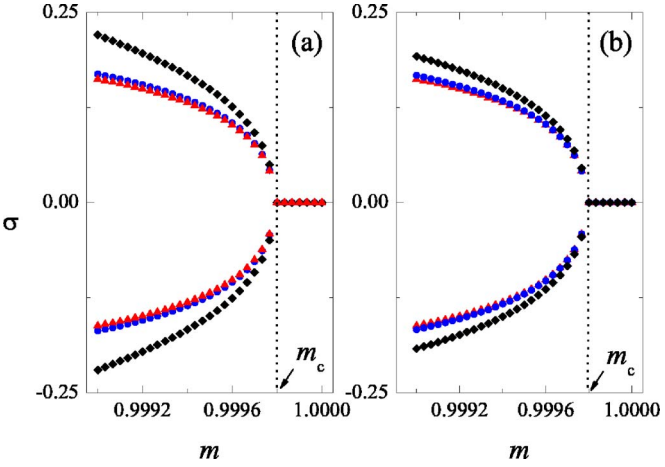

FIG. 4. (Color online) Bifurcation diagram of the (dimensionless) average velocity σ as a function of the (dimensionless) shape parameter m. (a) Number of rotators $N=5$ and three values of the coupling k_F: 0.2 (triangles), 0.1 (circles), and 0.06 (rhombs). (b) Coupling $k_F=0.2$ and three values of the number of rotators N: 5 (triangles), 7 (circles), and 8 (rhombs).

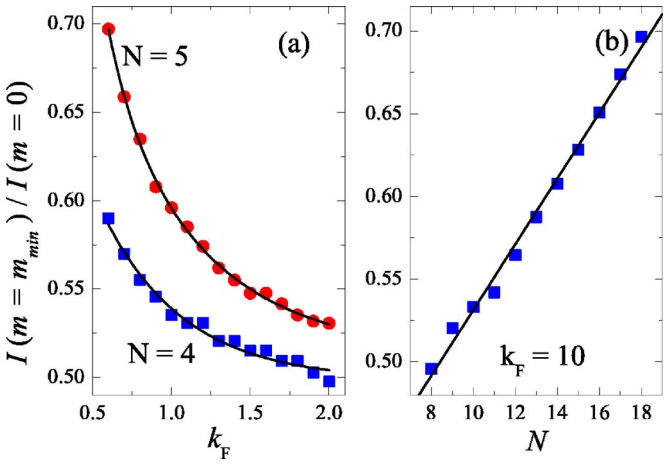

FIG. 5. (Color online) Normalized transmitted impulse associated with maximal desynchronization $I(m=m_{\min})/I(m=0)$ as a function of the coupling k_F for $N=4$ (squares) and $N=5$ (circles) rotators (a) and the number of rotators N for $k_F=10$ (b). Black lines denote exponential $[0.498\,14+0.281\,35\exp(-1.9322k_F)$, $0.512\,76+1.374\,78\exp(-k_F/0.166\,77)+0.366\,67\exp(-k_F/0.654\,32)$ for $N=4,5$, respectively] and linear $(0.332\,73+0.019\,86N)$ fits. The quantities plotted are dimensionless.

desynchronization (at $m_{\min}$) as this parameter is varied, provided the coupling is sufficiently large [hereafter referred to as the strong coupling (SC) regime]. Indeed, while increasing the shape parameter from 0 improves the desynchronization-induced regularization of the chain, in the sense that to optimize the frequency-locking to the forcing, it simultaneously increases the heterogeneity-induced desynchronization of the chain by increasing the amplitude dispersion on the one hand, and the reshaping-induced oscillation death on the other. Indeed, the latter effect becomes dominant for sufficiently narrow pulses: the equilibrium $(\theta_n, d\theta_n/d\tau)=(0,0)$, unstable when the rotators are uncoupled, becomes attracting and suppresses the $2T_F$ periodic oscillations via an inverse supercritical Hopf bifurcation [14]. Although the phenomenon of oscillation death is usually due to the interplay between high parameter dispersion and strong coupling [15], the present case provides an example where it remains in the weak coupling (WC) regime, as one observes in the instance shown in Fig. 4(a). There is a critical wave form corresponding to the shape parameter value $m_c \simeq 0.9998$, such that oscillation death occurs for $m \geqslant m_c$ and the complete chain becomes trivially synchronized irrespective of its size [cf. Fig. 4(b)]. This critical value coincides with that from which the above equilibrium becomes the resulting attractor for uncoupled rotators [13]. The dependence of the impulse transmitted at the pulse wave form corresponding to maximal desynchronization,

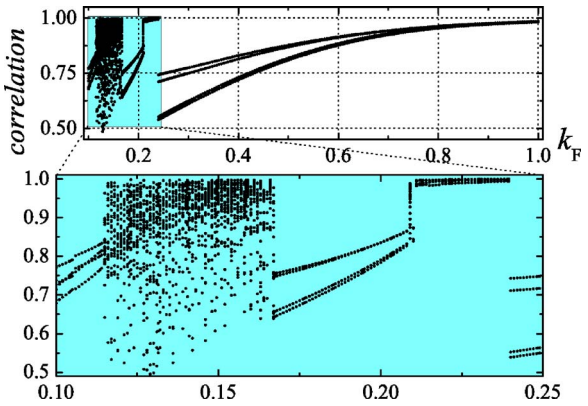

FIG. 6. (Color online) Bifurcation diagram of the correlation function as a function of the coupling for $N=5$ rotators and $m=0.5$. The expansion shows in detail the transitions associated with the WC regime. The quantities plotted are dimensionless.

$$I(m=m_{\min}) \equiv \int_0^{T_F} \mathrm{cn}^2(2K(m)\tau/T_F; m=m_{\min})d\tau, \quad (4)$$

on the coupling and the chain size is shown in Fig. 5. One typically finds an *exponential decay* law for the coupling dependence, and a *linear* law in the SC regime for the chain-size dependence. Since an exponential decay law is a universal hallmark of unstable systems, one expects the present one to remain valid for general damped, periodically driven arrays. The WC regime exhibits greater complexity, as can be seen in the instance shown in Fig. 6. Indeed, one typically finds windows where the chains present chaotic desynchronized states interspersed with windows containing regular states with different degrees of synchronization as well as abrupt transitions between them via crisis phenomena (see Fig. 6). Beyond the WC regime the synchronization of periodic states increases continuously as the coupling is increased.

To summarize, it has been shown that localized reshaping of the driving forces leads to transitions from chaotic to frequency-locked behavior in chains of dissipative coupled oscillators. It should be stressed that the above regularization scenario also occurs in two-dimensional arrays as well as in other coupled systems [16]. The present general mechanism to regularize chaotic arrays has potential applications in those cases where the intrinsic parameters of a system cannot be altered while any kind of periodic behavior is preferred to chaos, such as in superconducting Josephson arrays [17] or semiconductor laser arrays [18].

The author acknowledges financial support from the Spanish MCyT and European Regional Development Fund (FEDER) program through the FIS2004-02475 project.

[1] A. Pikovsky, M. G. Rosenblum, and J. Kurths, *Synchronization: A Universal Concept in Nonlinear Science* (Cambridge University Press, Cambridge, UK, 2001); S. Strogatz, *Sync: The Emerging Science of Spontaneous Order* (Hyperion, New York, 2003).

[2] R. Roy and K. S. Thornburg, Phys. Rev. Lett. **72**, 2009 (1994); A. V. Ustinov, M. Cirillo, and B. A Malomed, Phys. Rev. B **47**, 8357 (1993); K. Wiesenfeld, P. Colet, and S. H. Strogatz, Phys. Rev. Lett. **76**, 404 (1996); L. M. Floría and J. J. Mazo, Adv. Phys. **45**, 505 (1996).

[3] A. T. Winfree, *The Geometry of Biological Time* (Springer, New York, 2001); E. Mosekilde, Y. Maistrenko, and D. Postnov, *Chaotic Synchronization: Applications to Living Systems* (World Scientific, Singapore, 2002); D. Amit, *Modelling Brain Function* (Cambridge University Press, Cambridge, UK, 1989).

[4] S. H. Strogatz, Nature (London) **410**, 268 (2001).

[5] S. Boccaletti, J. Kurths, G. Osipov, D. L. Valladares, and C. S. Zhou, Phys. Rep. **366**, 1 (2002); R. Chacón, *Control of Homoclinic Chaos by Weak Periodic Perturbations* (World Scientific, London, 2005).

[6] Y. Braiman *et al.*, Phys. Lett. A **206**, 54 (1995); Y. Braiman, J. F. Lindner, and W. L. Ditto, Nature (London) **378**, 465 (1995); S. H. Strogatz, *ibid.* **378**, 444 (1995); J. F. Lindner, B. S. Prusha, and K. E. Clay, Phys. Lett. A **231**, 164 (1997); F. Qi, Z. Hou, and H. Xin, *ibid.* **308**, 405 (2003).

[7] A. Gavrielides *et al.*, Phys. Rev. E **58**, 5529 (1998); M. Weiss, T. Kottos, and T. Geisel, *ibid.* **63**, 056211 (2001); N. V. Alexeeva, I. V. Barashenkov, and G. P. Tsironis, Phys. Rev. Lett. **84**, 3053 (2000).

[8] R. Chacón, V. Preciado, and V. Tereshko, Europhys. Lett. **63**, 667 (2003).

[9] P. J. Martínez and R. Chacón, Phys. Rev. Lett. **93**, 237006 (2004); **96**, 059903(E) (2006).

[10] F. Qi, Z. Hou, and H. Xin, Phys. Rev. Lett. **91**, 064102 (2003).

[11] S. F. Brandt, B. K. Dellen, and R. Wessel, Phys. Rev. Lett. **96**, 034104 (2006).

[12] D. A. Steck, W. H. Oskay, and M. G. Raizen, Science **293**, 274 (2001).

[13] R. Chacón and A. Martínez García-Hoz, Phys. Lett. A **281**, 231 (2001); Phys. Rev. E **68**, 066217 (2003).

[14] See, e.g., S. H. Strogatz, *Nonlinear Dynamics and Chaos* (Addison-Wesley, Reading, MA, 1994), p. 249.

[15] Y. Yamaguchi and H. Shimizu, Physica D **11**, 212 (1984); G. B. Ermentrout, *ibid.* **41**, 219 (1990).

[16] R. Chacón (unpublished).

[17] R. S. Newrock *et al.*, Solid State Phys., Adv. Res. Appl. **54**, 263 (2000); B. R. Trees, V. Saranathan, and D. Stroud, Phys. Rev. E **71**, 016215 (2005).

[18] G. Kozyreff, A. G. Vladimirov, and P. Mandel, Phys. Rev. Lett. **85**, 3809 (2000).